Journal of Experimental Nanoscience
Publication details, including instructions for authors and subscription information:
http://www.informaworld.com/smpp/title~content=t716100757

Two modelling data analytical methods applied to optimise the preparation of norcantharidin chitosan nanoparticles

Wei Zhang[a]; Yang Liu[a]; Xiao-Yan Chen[a]; Yong-Yan Bei[a]; Jing-Yu Xu[a]; Wen-Juan Wang[a]; Xue-Nong Zhang[a]; Qiang Zhang[b]
[a] College of Pharmacy, Soochow University, Suzhou 215123, People's Republic of China [b] Department of Pharmaceutics, School of Pharmaceutical Science, Peking University, Beijing 100083, People's Republic of China

Online publication date: 05 July 2010

To cite this Article Zhang, Wei , Liu, Yang , Chen, Xiao-Yan , Bei, Yong-Yan , Xu, Jing-Yu , Wang, Wen-Juan , Zhang, Xue-Nong and Zhang, Qiang(2010) 'Two modelling data analytical methods applied to optimise the preparation of norcantharidin chitosan nanoparticles', Journal of Experimental Nanoscience, 5: 3, 271 — 284
To link to this Article: DOI: 10.1080/17458080903513284
URL: http://dx.doi.org/10.1080/17458080903513284

Journal of Experimental Nanoscience
Vol. 5, No. 3, June 2010, 271–284

Taylor & Francis
Taylor & Francis Group

Two modelling data analytical methods applied to optimise the preparation of norcantharidin chitosan nanoparticles

Wei Zhang[a], Yang Liu[a], Xiao-Yan Chen[a], Yong-Yan Bei[a], Jing-Yu Xu[a], Wen-Juan Wang[a], Xue-Nong Zhang[a]* and Qiang Zhang[b]

[a]*College of Pharmacy, Soochow University, Suzhou 215123, People's Republic of China;* [b]*Department of Pharmaceutics, School of Pharmaceutical Science, Peking University, Beijing 100083, People's Republic of China*

(*Received 2 June 2009; final version received 26 November 2009*)

In our study, the non-linear regression model and artificial neural networks (ANNs) were used to optimise the preparation of the loading norcantharidin chitosan nanoparticles (NPs) by ionic cross-linkage. Two major indexes, the particle size and the entrapment efficiency of the drug vehicles were synchronously optimised according to the normalised value calculated referring to the weights of the indexes and factors. For the purpose, a multiple regression model was constructed for fitting several preparation factors, including the low molecular weight of chitosan (LCS), sodium tripolyphosphate (TPP) concentrations and the temperature of the ionic cross-linkage reaction. Each of the level values in the factors was arranged using the $L_9(3^4)$ table and their linear weighted sum of the normalised value was taken as optimised object. A back-propagation (BP) network ($3 \times 7 \times 2$) in ANNs was created and trained for further checking the optimal results and the trained network was applied to simulate the experiment system and screen the optimal conditions. Finally, when the weights of temperature, particle size and entrapment efficiency were 0.1, 0.4 and 0.5, respectively, the best preparation condition of NPs was obtained as 131 ± 7 nm of particle size and 45.12% of entrapment efficiency at 40°C.

Keywords: chitosan; nanoparticles; non-linear regression; artificial neural networks

1. Introduction

Norcantharidin (NCTD) synthesised from cantharidin, an active constituent obtained from the dried body of the Chinese blister beetle (mylabris), is used as a traditional medicine in China, traced back to over 2000 years [1,2]. Clinical studies have shown that NCTD was effective against primary carcinoma of liver as an inhibitor of protein phosphatase 1 (PP1) and protein phosphatase 2A (PP2A), administered by oral and intravenous routes [3]. However, the clinical use of NCTD is limited because of the significant drawback of irritation of the urinary organs in previous cases [4]. In order

*Corresponding author. Email: zhangxuenong@163.com

ISSN 1745–8080 print/ISSN 1745–8099 online

DOI: 10.1080/17458080903513284
http://www.informaworld.com

to minimise its toxicity, several alternative preparations, such as microsphere, microemulsion, liposome and nanoparticle (NP) have been designed to improve the liver-targeting properties of NCTD [5].

The advantages of NPs as a powerful carrier and controlled release system were well known, which provided a potential ability for targeting the drug to some specified organs such as liver, spleen and brain [6–8]. The previous studies have shown that the targeting ability of NPs is closely related to the particle size – they are located in the liver when smaller than 200 nm [9]. For this reason, an incorporated NCTD–NPs may be suggested to modify its distribution and reduce the nephrotoxicity of NCTD.

Chitosan, as a non-toxic biodegradable polycationic polymer with low immunogenicity, has been extensively investigated as formula carrier and delivery system of therapeutic molecules such as genes, protein molecules, vaccines, cyclosporine A and ammonium glycyrrhizinate [10,11]. Chitosan NPs could be prepared by many methods, including the emulsion cross-linking, coacervation, spray-drying, emulsion-droplet coalescence, ionic gelation and self-assembled methods [12]. However, unlike poly (methacrylic acid and methacrylate) copolymer NPs, the larger particle size (>200 nm) of chitosan–TPP colloids could not address the need for targeting drug delivery [13]. For this aim, a low molecular weight chitosan (LCS, $8\sim10$ kDa) was selected to prepare the smaller size carrier loading NCTD chitosan–TPP NPs for improving the liver targeting characteristics [14].

Polynomial non-linear regression analysis had been used widely for establishing approximate mathematical models, wherein the variables and terms would be screened by the stepwise selection method according to the statistical significance [15,16], and the final model would be used to further analyse the relationship between factors and indexes. Instead of the modelling method, artificial neural networks (ANNs) have been applied to highly non-linear industrial processes as a powerful tool for approximating non-linear systems that are complex and difficult to identify simply based on the reaction phenomena [17,18]. It is generally argued that back-propagation (BP) network is the first type of the networks that is widely used for non-linear system analysis because of the clearly defined equations of correcting weights in networks [19].

Presently, orthogonal design has been used to evaluate the influence of different process factors on NPs' particles size and entrapment efficiency by non-linear regression analysis and ANNs [20,21]. The aim of this study is to develop a mathematical model and a BP network based on the orthogonal design in order to deduce the appropriate conditions for preparing the colloidal system with desirable properties of increasing the liver targeting and reducing the nephrotoxicity of NCTD.

2. Materials and methods

2.1. *Materials*

NCTD was purchased from Surui Medicine Chemical Industry Co. Ltd (Suzhou, China). Low molecular weight chitosan (LCS) with the deacetylation of 90.9% and molecular weight of 8–10 kDa was supplied by Xingcheng Biochemical Co. Ltd (Nantong, China). Sodium tripolyphosphate (TPP) was obtained from National Drug Group (Shanghai, China) and Pluronic F_{68} was purchased from Fluka Chemika (Switzerland).

Other chemicals and solvents were of analytical grades. Deionised twice-distilled water was used throughout the study.

2.2. *Preparation of NPs*

Chitosan NPs were prepared according to the procedure first reported by Calvo et al. [22], which was based on the ionic gelation of LCS with TPP anions and slightly modified. Briefly, LCS was dissolved in acetic acid aqueous solution containing NCTD of 0.4 mg/mL, and TPP aqueous solution was then added to the chitosan solution drop-by-drop under magnetic stirring, resulting in cross-linkage. After the reaction for 10 min, Pluronic F_{68} of 125 mg was dissolved in the solution as stabiliser. Aqueous solution of acetic acid (0.2% v/v), stirring rate (500 rpm), the mixed volume of chitosan and TPP (5 : 2, v/v) were kept at constant temperature. The temperature of the ionic cross-linkage reaction and the solution concentrations of LCS and TPP, as three factors, were constantly monitored. When the temperature was kept at 50°C, three kinds of phenomena were observed visually: solution, aggregates and opalescent suspension, and the zone of opalescent suspension (as shown in Figure 1) was further examined as NPs.

2.3. *Particle size analysis and morphological characterisation*

The analysis of particle size of NPs was performed by dynamic light scattering measured by Zetasizer Nanoparticle Analyser (Malvern Instruments Ltd., UK, range from 0.6 to 600 nm). The NP colloid samples were condensed using a Vivaflow 50 Ultrafilter (30,000 Da polysulfone resin filter membrane, Sartorius Co., Germany), and some of them were put into agar gel pipe (inter-diameter, 2 mm), solidified with glutaral for 24 h and embedded with osmium acid [23]. The morphological characteristics of nanoparticles were studied by transmission electron microscopy (TEM, JEM-1230, JEOL, Japan).

2.4. *Evaluation of drug entrapment efficiency and loading capacity*

An appropriate volume of NPs colloid was filtered through a 0.45 μm filter to remove non-soluble aggregate residues referring to the previous report [24,25]. The filtered colloid was then ultracentrifuged at 40,000 rpm for 45 min is an Optima MAX Centrifuge

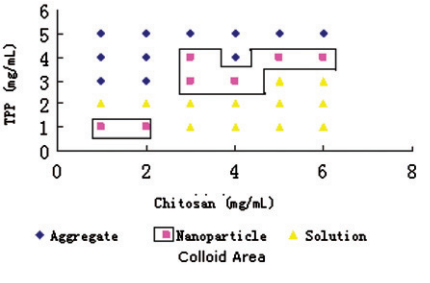

Figure 1. The concentration scope of chitosan NPs formation.

(Berkman Co. Ltd., USA). The supernatant was sampled and the concentration of NCTD in the supernatant was determined by a reversed-phase HPLC method.

Twenty microliters of supernatant were injected into a chromatograph equipped with a UV detector (Shimadzu LC-10AT, SPD-M10A, Japan) and a reversed-phase column (Hypersil ODS2, 4.6×250 mm, Elite, Dalian, China). The mobile phase was a mixture of acetonitrile: $H_2O = 10:90$ (adjusted to pH 3.1 by adding phosphoric acid), and the flow rate was 0.8 mL/min with the wavelength of 210 nm at 30°C. The NCTD entrapment efficiency (EE) and loading capacity (LC) were calculated as follows:

$$\mathrm{EE} = \frac{T - F}{T} \times 100\%$$

$$\mathrm{LC} = \frac{T - F}{W} \times 100\%.$$

T represents the total amount of NCTD in the colloid, F the free amount of NCTD in the supernatant, while W is the amount of NPs added.

2.5. *Experiment design*

Orthogonal design ($L_9(3^4)$) was applied to optimise the preparation of NPs, the particle size (nm) and drug entrapment efficiency (%) were estimated compositely by calculating the linear weighted sum of the normalised value. The level values of the factors affecting the characteristics of NPs were arranged in a three-level $L_9(3^4)$ table, in which the experimental points were distributed uniformly, and all the measurements were carried out in triplicate.

2.6. *Polynomial non-linear regression analysis*

According to the complexity in the reaction process, quadratic polynomial regression model was selected preliminarily to describe the relationship between factors and indexes, and the stepwise selection was used to choose significant variables in the model. To check the validity of the regression model, statistically significant F-ratios and correlation coefficients were applied. Finally, two regression equations about particle size and entrapment efficiency were obtained and they were also represented as two- (or three-) dimensional response plots for two (or three) variables at a time. The equation expressions of the indexes were normalised, respectively, according to the possible scopes of the indexes. The linear weighted sum of the normalised expressions was used to screen the optimal experiment conditions by simplex method [26,27].

2.7. *Artificial neural networks analysis*

BP network, which is applied frequently in ANNs, was created to simulate the experimental system, and trained through taking the factor values as network inputs and the index values as outputs. Especially, in hidden layer, the quantity of neurons was determined referring to Kolmogorov's law [28,29], and the training steps were confirmed by training error to avoid overtraining. It seemed that the experiment process became

a data NetBIOS, at least in data hierarchy, so that all the experimental results could be predicted by the trained network, and the optimal condition would be found out.

3. Results and discussion

The orthogonal design is a kind of fractional factor design allowed to test multiple independent process variables within a single experiment, and offers the possibility of investigating multivariables at different levels, simply performing a limited number of experiments. The variables are chosen through taking into account other reports on chitosan–TPP NP preparation and the results of our preliminary experiments.

Since the procedure was first reported by Calvo et al., almost all the chitosan NPs were prepared at room temperature (25°C). However, our study indicated that the reaction temperature exercised a great influence on particle size, drug entrapment percentage and even whether or not NPs could form, and it was identified in the preliminary experiments that the NPs formation temperature ranged from approximately 40°C to 60°C. It was probably because that low molecular weight chitosan was not as easy to crosslink at room temperature as the high molecular weight one, which was often used [30]. The concentration zones of solution, aggregates and opalescent suspension at reaction temperature of 50°C are shown in Figure 1. Visually, there are two zones forming NP colloid and the particle size in the zone of low concentration (100–300 nm) is smaller than the high concentration, detected using Zetasizer Nanoparticle Analyser (Malvern Instruments Ltd., UK). Therefore, the low-concentration zone, including the concentration range of TPP (0.6–1.2 mg/mL) and LCS ($1 \sim 2$ mg/mL), is investigated (Tables 1 and 2).

The following quadratic polynomial regression model, usually applied to describe some complex processes, was generated for the statistical analysis of the results:

$$Y = a_0 + a_1X_1 + a_2X_2 + a_3X_3 + a_4X_1^2 + a_5X_2^2 + a_6X_3^2 + a_7X_1X_2 + a_8X_1X_3 + a_9X_2X_3 \quad (1)$$

where Y represents the mean particle size or entrapment percentage, X_i the independent variables: LCS concentration (X_1), TPP concentration (X_2), temperature (X_3) and a_i ($i = 1, 2, 3, \ldots, 6$) represent constants.

Stepwise selection is used to choose significant terms (variables), and statistically significant levels ($\alpha = 0.05$), critical values of leading variables ($F_a = 0.05$) and deleting variables ($F_e = 0.05$) are set so that two regression equations could be obtained as follows:

$$PS(\text{nm}) = -1880 + 1240X_1 - 878X_2 + 62X_3 - 256X_1^2 + 422X_2^2 - 0.468X_3^2 - 8.9X_1X_3 \quad (2)$$

Table 1. The level values of the factors affecting NPs in $L_9(3^4)$.

Levels	LCS (mg/mL)	TPP (mg/mL)	Temperature (°C)
1	1	0.6	40
2	1.5	0.9	50
3	2	1.2	60

Table 2. Experimental results.

Experiment number	LCS x_1 (mg/mL)	TPP x_2 (mg/mL)	Temperature x_3 (°C)	Mean particle size (nm)	Entrapment percentage (%)
1	1 (1)	0.6 (1)	40 (1)	113 ± 7	29.26 ± 3.73
2	1 (1)	0.9 (2)	50 (2)	125 ± 12	11.34 ± 1.71
3	1 (1)	1.2 (3)	60 (3)	155 ± 22	29.51 ± 3.33
4	1.5 (2)	0.6 (1)	50 (2)	286 ± 29	24.89 ± 2.29
5	1.5 (2)	0.9 (2)	60 (3)	196 ± 12	18.27 ± 3.40
6	1.5 (2)	1.2 (3)	40 (1)	138 ± 7	16.63 ± 1.70
7	2 (3)	0.6 (1)	60 (3)	149 ± 19	29.79 ± 2.01
8	2 (3)	0.9 (2)	40 (1)	140 ± 6	44.77 ± 2.45
9	2 (3)	1.2 (3)	50 (2)	175 ± 18	54.64 ± 3.71

PS is particle size, and the multiple correlation coefficient is $R = 0.9797$.

$$EE(\%) = 213 - 65.6X_1 - 378X_2 + 38.9X_1^2 + 104X_2^2 + 47.2X_1X_2 - 1.33X_1X_3 + 2.38X_2X_3 \quad (3)$$

EE is entrapment percentage, and the multiple correlation coefficient is $R = 0.9987$.

The two- (three-) dimensional response plots on the factor-index are shown in Figure 2, which illustrates the effect of the LCS and TPP concentrations and temperature on particle size, and Figure 3 demonstrates the effect on entrapment percentage. Obviously, the effect of these factors on the particle size is different from the entrapment percentage, comparing Figures 2 and 3, and in all probability, smaller particle would mean lower entrapment percentage. In Figure 2, the trends following the knees of curves could be accounted by forming a mixture of NPs and aggregates, and in Figure 3, the entrapment percentage increases with the LCS (or TPP) concentration and temperature. In view of the different variations between PS and EE, the optimisation is in need of coordinating PS and EE through the following analysis.

The parameters set to perform the experiment optimisation are shown in Table 3, where lower/upper bounds are the potential ranges of factors (or indexes) based on the preliminary experimental results, desirable direction is the anticipant orientation of optimisation (+1 or −1 mean that larger or smaller values are expected, respectively, and 0 represents having no desirable direction), and weights (the sum is 1) represent the significance of factors (or indexes).

Concerning the joint effects of factors and the integrated requirement of PS and EE, the linear weighted sum of the normalised values should be calculated to solve the problem according to the following formula:

$$F(X_1, X_2, X_3) = \sum_{i=1}^{m+n} D \frac{F_i - F_{\mathrm{mid}\,i}}{F_{\max i} - F_{\min i}} W_i \ (i = 1, 2, \ldots, m+n) \quad (4)$$

where m and n are the quantities of factors and indexes, respectively, D the desirable direction value, F_i the factor/index expressions ($F_{\mathrm{mid}\,i}$, $F_{\max i}$ or $F_{\min i}$ is the middle, maximum or minimum value in the range from the lower bounds to the upper ones.)

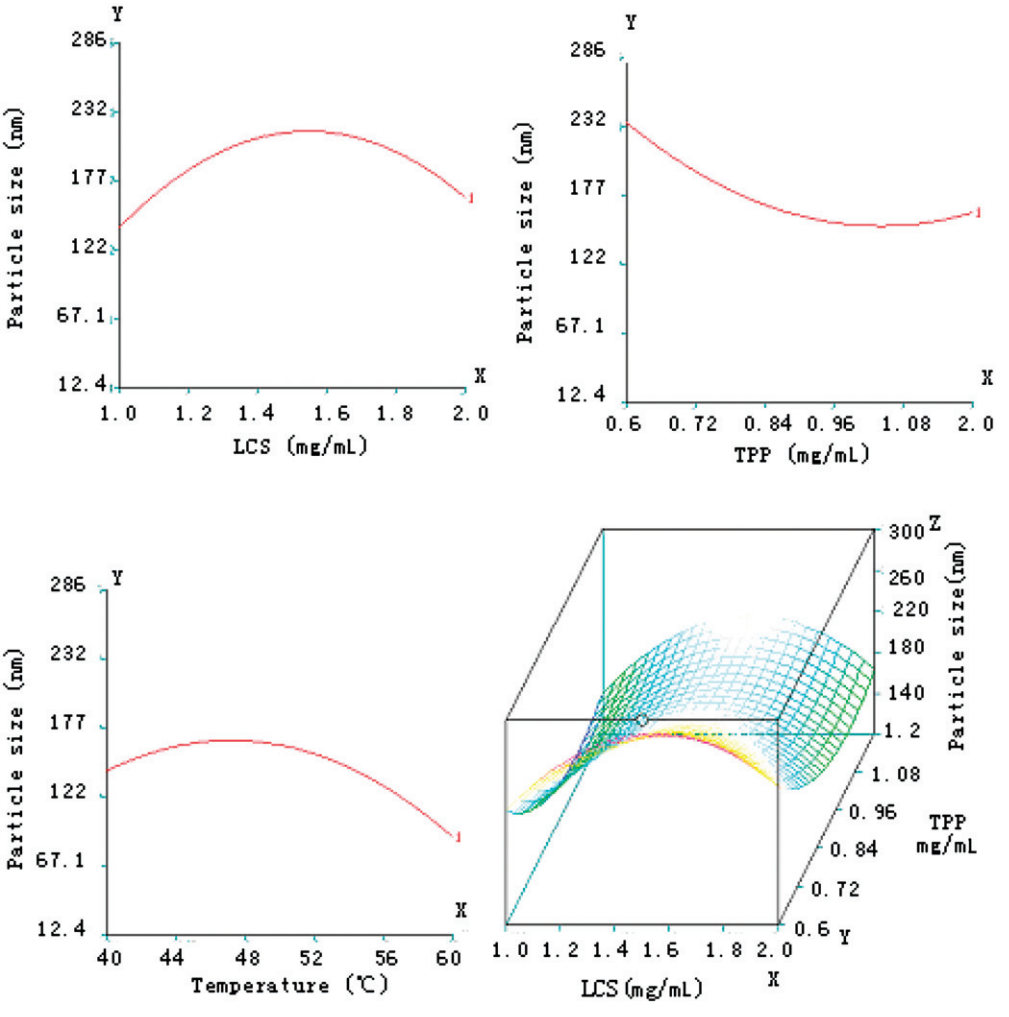

Figure 2. Two-dimensional/three-dimensional curve line/response surface plots showing the variation in the NP size (nm) with changes in LCS and TPP concentrations and the reaction temperature.

and W_i the weight of the factors (or indexes). In order to achieve smaller PS, larger EE and lower temperature synchronously, it is necessary to calculate the maximum of the function (4) using simplex method. When the maximum could be acquired, the optimal conditions, the values of X_1, X_2 and X_3 could be obtained: the LCS and TPP concentrations (5 : 2 v/v) are 2 and 1.1 mg/mL, and the temperature is 40°C. Meanwhile, the particle size of 143 nm and the entrapment percentage of 53.2% could also be predicted based on the functions (2) and (3).

In general, most of the technical processes are highly non-linear systems, which are in need of complex modelling techniques, and a lot of mathematical models have been used to analyse multivariable non-linear ones, while the appropriate models are usually

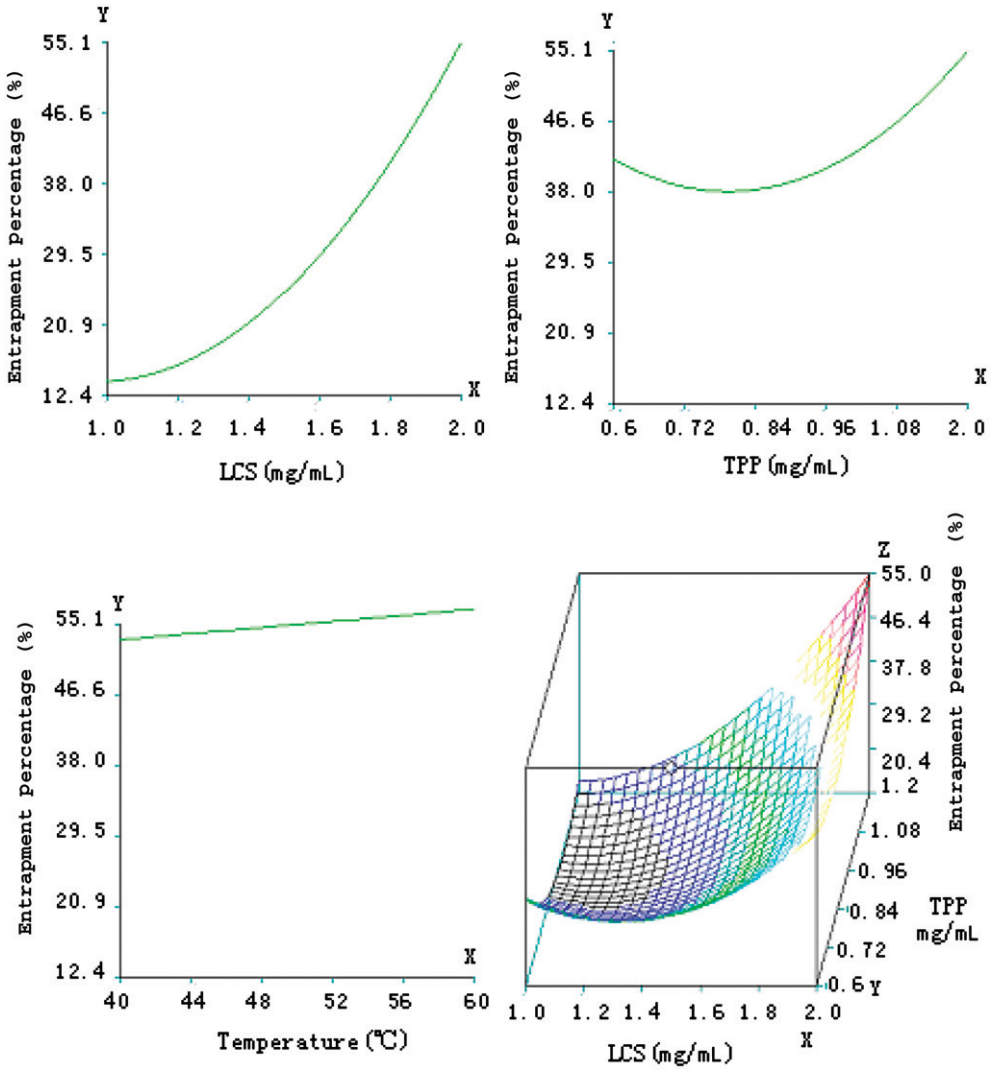

Figure 3. Two-dimensional/three-dimensional curve line/response surface plots showing the variation in the drug encapsulation percentage with changes in LCS and TPP concentration and temperature.

Table 3. Setting parameters for synchronous optimisation.

Terms	Lower bound	Upper bound	Desired direction	Weight
LCS (mg/mL)	1.0	2.0	0	–
TPP (mg/mL)	0.6	1.2	0	–
Temperature (°C)	40	60	−1	0.1
PS (nm)	100	300	−1	0.5
EE (%)	0	60	1	0.4

complicated, inaccurate and difficult to obtain. So, the quadratic polynomial regression model likely caused the optimisation error because of inaccuracy. For further checking the result, the neural networks, eliminating the need for modelling, are often used as simulating tools because of the ability to fit a variety of input–output patterns; the BP network is often a better selection as the first type of ANNs that is extensively used for simulating non-linear systems.

In this study, a BP network is created using Matlab 7.0 (MathWorks, Inc., USA) after the preparation according to orthogonal design $L_9(3^4)$, and the level values of three factors are selected as input and the values of two indexes as output [31]. Because of the inequality among the order of magnitude of samples (input and output), the original data should be normalised as follows:

$$X_i = \frac{x_i - x_{\min}}{x_{\max} - x_{\min}}$$

where x_i, $x_{\min}$ and $x_{\max}$ are the original, minimum and maximum values of the factors (or indexes) and X_i represents the normalised value of x_i.

Single hidden layer network, containing three input neurons and two output ones according to the quantities of factors and indexes, was selected as an analogue of the experiment, because it was flexible enough to fit non-linear mapping. According to Kolmogorov's law, the hidden layer in the network could contain seven neurons (the whole network structure ($3 \times 7 \times 2$) is shown in Figure 4), in which X_1, X_2, X_3, PS and EE are the normalised values of the LCS and TPP concentrations, temperature, particle size and entrapment percentage, respectively. The training for 500 times, determined by several more training, is carried out in the BP network and the transfer function in the hidden layer is set as 'tansig'. The other parameters, such as the transfer function of the

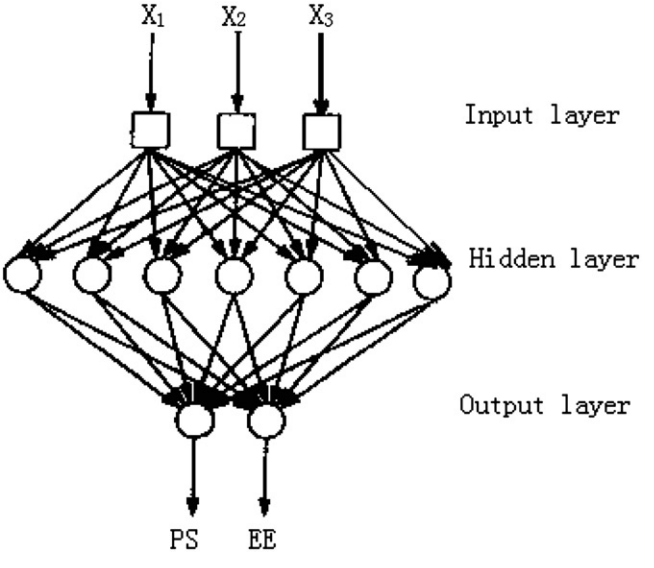

Figure 4. The back-propagation (BP) network structure ($3 \times 7 \times 2$).

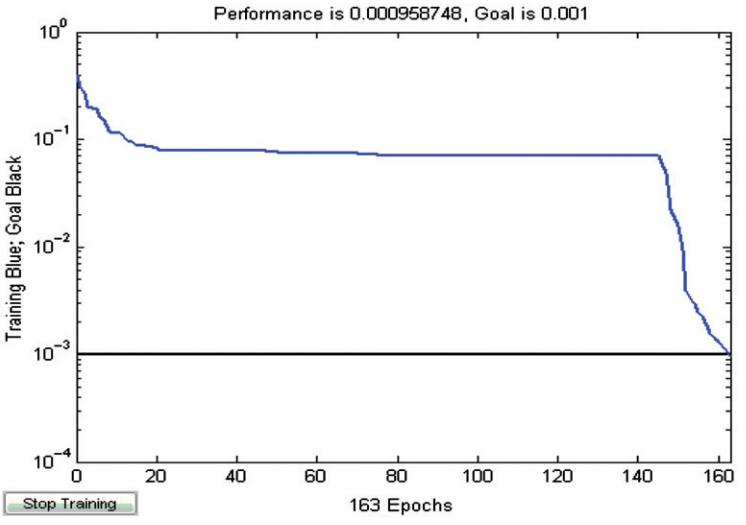

Figure 5. The training result of the network in Matlab 7.0.

output layer and the training function of the network, are set as 'logsig' and 'trainlm' (Levenberg–Marquardt BP training function) in Matlab 7.0, and the training result is shown in Figure 5. After training for 163 times, the network mean square error (MSE), which is often used to evaluate the network performance, has reached 0.000959 (the goal is 0.001), and it could be deduced that the network is accurate enough to predict other experimental results.

The network trained could be applied to predict and search for the optimal preparation condition of chitosan NPs. In the beginning, the step width of three factors (LCS, TPP and temperature) are set as 0.1, 0.1 and 5, so that there are $11 \times 7 \times 5$ sets of combination values of experiment conditions, which are normalised and input to network. Finally, all the experimental results are predicted, and the optimal condition: the LCS and TPP concentrations (5 : 2 v/v) of 2 and 1.0 mg/mL, and temperature of 40°C (almost identical to the result of polynomial non-linear regression analysis) would be found out by a simple Matlab program based on the function (4) and the settings in Table 3. Meanwhile, the particle size of 131.46 nm and the entrapment percentage of 53.47%, under the optimal condition, are well predicted.

Zetasizer Nanoparticle Analyser is used to measure the mean particle size, and the particle size distribution is shown in Figure 6, in which it is observed the average particle size of 127.2 nm. The entrapment percentage is detected by HPLC (referring to 2.5), so that the entrapment efficiency of 45.12% and the loading capacity of 7.3% are obtained. The low-drug contents could be aptly accounted by the high-aqueous solubility of NCTD, resulting in considerable drug loss to the aqueous medium.

TEM images, the photos of NPs stained with 2% phosphotungstic acid and the ones not stained are shown in Figure 7 and used to evaluate if the NP forms and the cross-linkage process take place by charge in the preparation condition. The spheres in the images illustrate that chitosan–TPP NPs have formed, and the particle sizes in

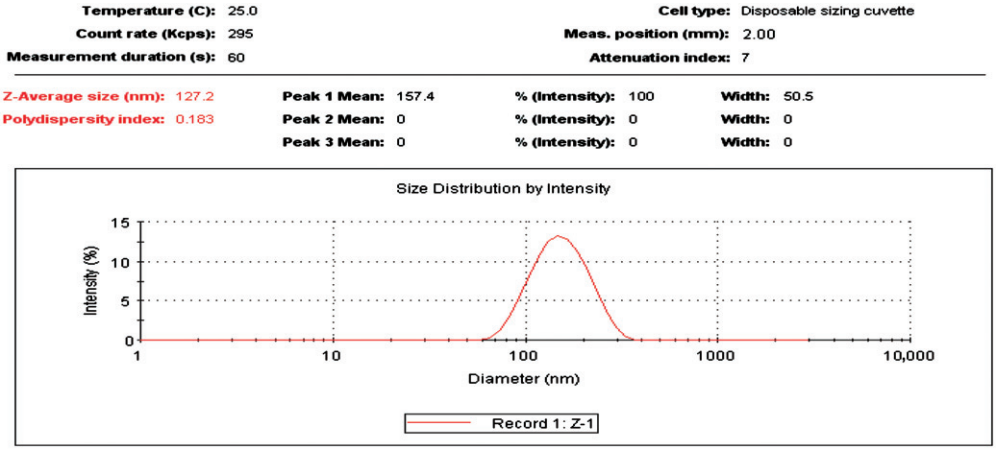

Figure 6. Particle size distribution analysis.

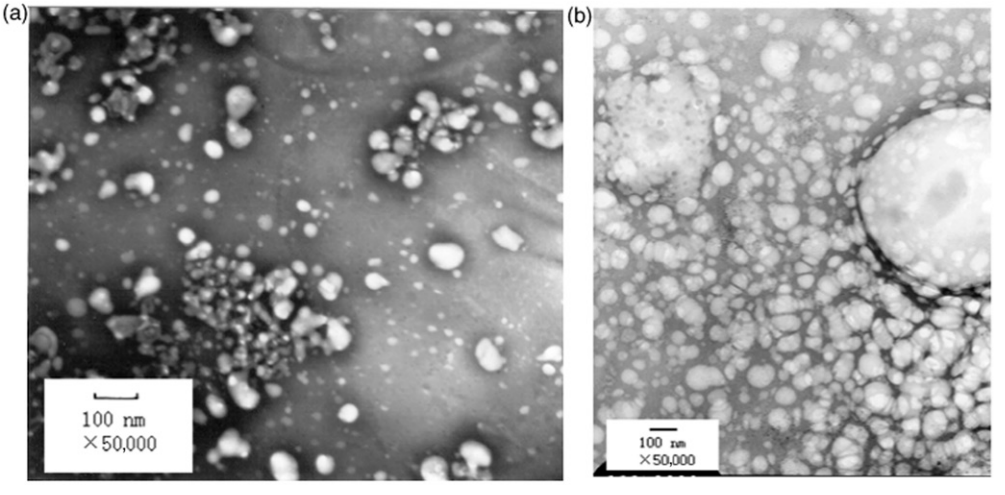

Figure 7. TEM images of low molecular weight chitosan (LCS) NPs loading NCTD: (a) the NPs stained with 2% phosphotungstic acid; (b) the unstained NPs.

Figures 6 and 7 are in substantial agreement, while the NPs stained are little smaller than the not stained ones, which is probably because of the acidic condition of 2% phosphotungstic acid that prevents NP aggregation.

From the results, the optimal condition is screened out by two data analysis approaches. Since particle size and entrapment were taken into consideration simultaneously as per the function (4), it is obvious that the optimal formulations were superior to the nine formulations in $L_9(3^4)$ table. Previously, it was only single index (particle size or entrapment) that could be optimised by traditional methods [32]. The smallest particle size of 100.7 nm exhibited 10.11% of entrapment, when the LCS and TPP concentrations

were 1 and 0.9 mg/mL and the temperature was 40°C. Also, the largest entrapment of 54.7% with the particle size of 175 nm was obtained when the LCS and TPP concentrations were 2 and 1.2 mg/mL and the temperature was 50°C (the 9th formulation in Table 2). This result was unable to attend to particle size and entrapment at one time, so it was reasonable that the optimal formulation was still superior to it. However, modelling predictions arose some deviations, which could be explained by the inaccurate math-model of polynomial non-linear regression analysis and the poor data used to train the network. So, it is probably a better choice to apply two methods to cross-reference.

4. Conclusions

As a general conclusion, the relationship of index and factor could be described precisely by mathematical modelling, and it is not necessary to collect enormous experimental data to establish an accurate analytical model. On the contrary, the non-math-modelling technique (ANNs) is often applied to simulate experimental system through creating accurate network instead of searching or establishing a complicated math model. The quality of network depends on the quantity of the training samples and influences the precision of analysis. The advantages of the two methods could complement each other to solve problems. On the other hand, introducing the linear weighted sum of the normalised value makes it possible to optimise multiple indexes at one time. So they were superior to the traditional method.

In general, the modelling data analytical methods could also be applied to analyse those data from many other experimental designs, such as rotatable central composite design or uniform design, available reference approaches; the analytical processes are the same as specified above.

Acknowledgements

This work was supported by the National Key Technology R&D Program in the 11th Five Year Plan of China (2006BAI09B00), the Innovation Fund of Medium or Small Science and Technology Enterprises, the National Science and Technology Ministry (07C26223201333), Social Development Foundation of Jiangsu Province (BS2005022), the High New Technology Research Project from the Department of Education of Jinagsu Province (JHB05-46) and grants from the Health Department of Jinagsu Province (H200630).

References

[1] G.S. Wang, *Medical uses of mylabris in ancient China and recent studies*, J. Ethnopharmacol. 26 (1989), pp. 147–162.

[2] X. Liu, W.S. Heng, A. Paul, Q. Li, and L.W. Chan, *Novel polymeric microspheres containing norcantharidin for chemoembolization*, J. Control Release 116 (2006), pp. 35–41.

[3] X.H. Liu, I. Blazsek, M. Comisso, S. Legras, S. Marion, P. Quittet, A. Anjo, G.S. Wang, and J.L. Misset, *Effects of norcantharidin, a protein phosphatase type-2A inhibitor, on the growth of normal and malignant haemopoietic cells*, Eur. J. Cancer 31A (1995), pp. 953–963.

[4] G.S. Wang, *Hydrolyze of norcantharidin and subtracting methyla alleviate stimulation of renal system*, Chin. Pharm. Bull. 18 (1983), pp. 18–20.

[5] L.X. Wang, H.B. He, X. Tang, R.Y. Shao, and D.W. Chen, *A less irritant norcantharidin lipid microspheres: Formulation and drug distribution*, Int. J. Pharm. 323 (2006), pp. 161–167.
[6] R. Gref, Y. Minimitake, M.T. Peracchia, V.T.-B. Skoy, V. Torchilinm, and R. Langer, *Biodegradable long-circulating polymeric nanospheres*, Science 18 (1994), pp. 1600–1603.
[7] M. Gaumet, A. Vargas, R. Gurny, and F. Delie, *NPs for drug delivery: The need for precision in reporting particle size parameters*, Eur. J. Pharm. Biopharm. 8 (2007), pp. 1–9.
[8] R. Gref, M. Lück, P. Quellec, M. Marchand, E. Dellacherie, S. Harnisch, T. Blunk, and R.H. Müller, *Stealth' corona-core NPs surface modified by polyethylene glycol (PEG): Influences of the corona (PEG chain length and surface density) and of the core composition on phagocytic uptake and plasma protein adsorption*, Colloids Surf. B Biointerfaces 18 (2000), pp. 301–313.
[9] S.M. Moghimi and R. Rajabi-Siahboomi, *Advanced colloid-based systems for efficient delivery of drugs and diagnostic agents to the lymphatic tissues*, Prog. Biophys. Mol. Biol. 65 (1996), pp. 221–249.
[10] J.L. Chewa, C.B. Wolfowicz, H.Q. Mao, K.W. Leong, and K.Y. Chua, *Chitosan NPs containing plasmid DNA encoding house dust mite allergen, Der p1 for oral vaccination in mice*, Vaccine 21 (2003), pp. 2720–2729.
[11] Y. Wu, W.L. Yang, C.C. Wang, J.H. Hu, and S.K. Fu, *Chitosan NPs as a novel delivery system for ammonium glycyrrhizinate*, Int. J. Pharm. 295 (2005), pp. 235–245.
[12] X.Q. Wang, J.D. Daia, C. Zhen, Z. Tao, G.M. Xia, T. Nagaic, and Q. Zhang, *Bioavailability and pharmacokinetics of cyclosporine A-loaded pH-sensitive NPs for oral administration*, Int. J. Pharm. 97 (2004), pp. 421–429.
[13] K.A. Janes, P. Calvo, and M.J. Alonso, *Polysaccharide colloidal particles as delivery systems for macromolecules*, Adv. Drug Deliv. Rev. 47 (2001), pp. 83–97.
[14] A. Vila, A. Sánchez, K. Janes, I. Behrens, T. Kissel, J.L. Vila-Jato, and M.J. Alonso, *Low molecular weight chitosan nanoparticles as new carriers for nasal vaccine delivery in mice*, Eur. J. Pharm. Biopharm. 57 (2004), pp. 123–131.
[15] A.J. Miller, *Selection of subsets of regression variables (with discussion)*, J. R. Stat. Soc. Ser. A 147 (1984), pp. 389–425.
[16] M. Janet and G. Daniel, *Stepwise selection of variables in data envelopment analysis: Procedures and managerial perspectives*, Eur. J. Oper. Res. 180 (2007), pp. 57–67.
[17] A.E. Farell and S.D. Roat, *Framework for enhancing fault diagnosis capabilities of artificial neural networks*, Comput. Chem. Eng. 18 (1994), pp. 613–635.
[18] K. Meert, *Estimation of the average chain length of polymers with neural classifiers*, Proceedings of the IEEE International Conference on Neural Networks '94, Orlando, FL (1994), pp. 3822–3827.
[19] D.E. Rumelhart, G.E. Hinton, and R.J. Williams, *Learning internal representation by error propagation*, in *Parallel Distributed Processing: Exploration in the Microstructure of Cognition*, Vol. 1, D.E. Rumelhart and J.L. McClelland, eds., MIT, Cambridge, 1986, pp. 318–362.
[20] J. Peng, F. Dong, Q. Xu, Y. Xu, Y. Qi, X. Han, L. Xu, G. Fan, and K. Liu, *Orthogonal test design for optimization of supercritical fluid extraction of daphnoretin, 7-methoxy-daphnoretin and 1, 5-diphenyl-1-pentanone from Stellera chamaejasme L. and subsequent isolation by high-speed counter-current chromatography*, J. Chromatogr. A 1135 (2006), pp. 151–157.
[21] V. Mandal, Y. Mohan, and S. Hemalatha, *Microwave assisted extraction of curcumin by sample–solvent dual heating mechanism using Taguchi L9 orthogonal design*, J. Pharm. Biomed. Anal. 46 (2008), pp. 322–327.
[22] P. Calvo, C. Remuñan-López, J.L. Vila-Jato, and M.J. Alonso, *Chitosan and chitosan/ethylene oxide-propylene oxide block copolymer NPs as novel carriers for proteins and vaccines*, Pharm. Res. 14 (1997), pp. 1431–1436.
[23] X.N. Zhang, L.H. Tang, J.H. Gong, X.Y. Yan, and Q. Zhang, *An alternative albendazole polybutylcyanoacrylate nanoparticles preparation, pharmaceutical properties and tissue distribution*, Lett. Drug Des. Discov. 3 (2006), pp. 275–280.

[24] J.D. Dai, T. Nagai, X.Q. Wang, T. Zhang, M. Meng, and Q. Zhang, *pH-sensitive nanoparticles for improving the oral bioavailability of cyclosporine A*, Int. J. Pharm. 280 (2004), pp. 229–240.
[25] X.N. Zhang, L.H. Tang, J.H. Gong, X.Y. Yan, and Q. Zhang, *An alternative paclitaxel self-emulsifying microemulsion formulation: Preparation, pharmacokinetic profile and hypersensitivity evaluation*, PDA J. Pharm. Sci. Tech. 60 (2006), pp. 89–94.
[26] M. Atencia, G. Joya, and F. Sandoval, *Dynamical analysis of continuous higher-order hopfield networks for combinatorial optimization*, Neural Comput. 171 (2005), pp. 802–1819.
[27] M. Liu and S. Zhang, *An LMI approach to design H (infinity) controllers for discrete-time nonlinear systems based on unified models*, Int. J. Neural Syst. 18 (2008), pp. 443–452.
[28] M. Abud-Archila, D.G. Va'zquez-Mandujano, M.A. Ruiz-Cabrera, A. Grajales-Lagunes, M. Moscosa-Santilla'nb, L.M.C. Ventura-Canseco, F.A. Gutie'rrez-Miceli, and L. Dendooven, *Optimization of osmotic dehydration of yam bean (Pachyrhizus erosus) using an orthogonal experimental design*, J. Food Eng. 84 (2007), pp. 413–419.
[29] L. Guo, S.Y. Cho, S.S. Kang, S.-H. Lee, H.-Y. Baek, and Y.S. Kim, *Orthogonal array design for optimizing extraction efficiency of active constituents from Jakyak-Gamcho decoction, the complex formula of herbal medicines, Paeoniae Radix and Glycyrrhizae Radix*, J. Ethnopharmacology 113 (2007), pp. 306–311.
[30] M. Bivas-Benita, M. Laloup, S. Versteyhe, J. Dewit, J. De Braekeleer, E. Jongert, and G. Borchard, *Generation of Toxoplasma gondii GRA1 protein and DNA vaccine loaded chitosan particles: Preparation, characterization, and preliminary in vivo studies*, Int. J. Pharm. 266 (2003), pp. 17–27.
[31] K. Hornik, M. Stinchcombe, and H. White, *Multilayer feedforward networks are universal approximators*, Neural Netw. 2 (1989), pp. 359–366.
[32] Y. Aktas, K. Andrieux, and M.J. Alonso, *Preparation in vitro evaluation of chitosan nanoparticles containing a caspase inhibitor*, Int. J. Pharm. 298 (2005), pp. 378–383.